Pergamon

J. Aerosol Sci., Vol. 26, No. 4, pp. 547–558, 1995

0021-8502/95 $9.50 + 0.00

0021-8502(94)00134-0

AEROSOL FORMATION IN DIFFUSIVE BOUNDARY LAYER: BINARY HOMOGENEOUS NUCLEATION OF AMMONIA AND WATER VAPOURS

M. Kulmala,* H. Vehkamäki,* T. Vesala,* J. C. Barrett† and C. F. Clement‡

*Department of Physics, P.O. Box 9, FIN-00014 University of Helsinki, Finland
†D.N.S.T., Royal Naval College, Greenwich, London SE 10 9 NN, U.K.
‡15 Witan Way, Wantage, Oxon OX12 9 EU, U.K.

(*First received* 13 *June* 1994; *and in final form* 26 *September* 1994)

Abstract—The formation of aerosol particles from ammonia–water vapour system by homogeneous binary nucleation has been studied. Numerical simulations based on the standard classical nucleation theory, self-consistent correction and the revised (original) classical nucleation theory are performed and they show that significant nucleation can occur in the boundary layer of an evaporating ammonia droplet in a humid atmosphere. The temperature of the ammonia droplet is below its boiling point. If the temperature of humid air is 40–50°C greater than the droplet temperature, significant droplet formation will occur.

INTRODUCTION

Considerable quantities of toxic and flammable gases are commonly used by many types of industrial installations. Many hazardous gases are stored and transported in bulk in liquid form, under pressure at atmospheric temperature or refrigerated at their boiling point (see e.g. Kukkonen, 1990). Serious hazard to the public may be caused in possible accidental releases of these substances. Reliable computational methods are therefore needed for estimating possible accidental release rates and the atmospheric dispersion of substances. Recently, Kukkonen *et al.* (1989) and Vesala and Kukkonen (1992) have studied the effect of aerosol dynamics (specially evaporation of ammonia droplets) on release rates.

In our recent work (Barrett *et al.*, 1992) we have studied aerosol formation in diffusive boundary layer, where large vapour supersaturations can arise. As a practical example, we examined formation of water droplets in the boundary layer of an evaporating ammonia droplet in the humid atmosphere. The flows of vapours and heat have earlier been studied quite extensively (Vesala, 1991). The surface temperature of a droplet is typically 70°C lower than the ambient temperature. In the situation considered water flows towards droplets and ammonia outwards. Since Barrett *et al.* (1992) studied only homogeneous homomolecular nucleation and we have a binary vapour system, we consider in the present study the binary homogeneous nucleation as a next step.

In the present work we study homogeneous heteromolecular nucleation of NH_3 and water vapours using standard and revised classical nucleation theories in numerical simulations. Also the self-consistency correction to the classical theory is used. A comparison between the two theories is performed. One should notice that the classical nucleation theory has its limitations (macroscopic properties, capillarity approximation), which are not considered here. The purpose of this study is to examine in what conditions ammonia–water liquid aerosols can be generated at boundary layers of evaporating ammonia droplets by heteromolecular nucleation.

BINARY NUCLEATION

According to the general formula of statistical physics the probability of a fluctuation producing a condensation nucleus is proportional to $\exp(-\Delta G^*/kT)$, where ΔG^* is the minimum work needed to form the nucleus, k is the Boltzmann constant and T is

temperature in Kelvins. The nucleation rate I can be predicted as

$$I = C \exp \frac{-\Delta G^*}{kT}, \tag{1}$$

where C is a (mainly) kinetic factor. It can be shown (e.g. Reiss, 1950; Heist and Reiss, 1974) that in the three-dimensional space $(n_W, n_A, \Delta G)$, where n_i denotes the number of molecules of species i in the cluster, there exists a saddle point which corresponds to the minimum height of the free energy barrier, or $\Delta G^* = \Delta G_{sp}$ (sp is the saddle point). Once a cluster reaches the saddle point, nucleation takes place and the cluster can grow to a larger droplet. Hence, the radius and composition at this point (denoted by r^*, n_w^*, n_a^*) are called critical or equilibrium values. The standard and the revised version of the classical theory give different saddle point compositions.

The standard classical model

The Gibbs free energy of formation of a liquid cluster in a binary mixture of vapours can be given by the expression (e.g. Yue and Hamill, 1979)

$$\Delta G(n_w, n_a) = -n_W kT \ln \frac{A_{Wg}}{A_{Wl}} - n_A kT \ln \frac{A_{Ag}}{A_{Al}} + 4\pi r^2 \sigma, \tag{2}$$

where r is the radius of the cluster and σ is the surface tension. For the special systems of water and ammonia vapours, W refers to water and A refers to ammonia. We have used the following quantities: $A_{Wg}\,(p_W/p_{Ws})$ is the water activity in the gas phase, which corresponds to the saturation ratio of water in the homomolecular system; $A_{Ag}\,(p_A/p_{As})$ the ammonia activity in the gas phase, which corresponds to the saturation ratio of ammonia in the homomolecular system; $A_{Wl}\,(p_{W,sol}/p_{Ws})$ the water activity in the liquid phase, and $A_{Al}\,(p_{A,sol}/p_{As})$ the ammonia activity in the liquid phase. p_W and p_A are the respective partial pressures of water and ammonia vapour, p_{Ws} and p_{As} are the respective equilibrium vapour pressures of water and ammonia vapour over a flat surface of pure substance, and $p_{i,sol}$ is the partial vapour pressure of species i over a flat surface of the solution.

The radius r is given by $\frac{4}{3}\pi r^3 \rho = n_W m_W + n_A m_A$, where ρ is the density of the solution, m_W is the mass of a water molecule and m_A is the mass of an ammonia molecule.

The nucleation rate is (Stauffer, 1976)

$$I = R_{AV} F Z e^{-\Delta G^*/kT}, \tag{3}$$

where R_{AV} is an average condensation rate and Z is the Zeldovich non-equilibrium factor (for details see Kulmala and Laaksonen, 1990). F is the total number of clusters including monomers and is given by

$$F = N_{W0} + N_{A0} + \sum_A \sum_A N_{AW}, \tag{4}$$

where N_{A0} and N_{W0} are the numbers of single molecules of A and W present, and N_{AW} is the number of clusters containing n_A, n_W molecules.

The self-consistency correction

The self-consistency correction (scc) to the standard classical theory has been adopted from Kulmala *et al.* (1992). The nucleation rate I can be calculated from equation (3). The Gibbs free energy at the saddle point is given as

$$\exp\left(-\frac{\Delta G^*_{scc}}{kT}\right) = \exp\left(-\frac{\Delta G^*}{kT}\right) \times \frac{\exp((36\pi)^{1/3(\sigma/kT)}[(1-X)v_W + Xv_A]^{2/3})}{(A_{Wg}/A_{Wl})^{1-X} \times (A_{Ag}/A_{Al})^X}. \tag{5}$$

Here v_i is the partial molecular volume of molecule i, and X the mole fraction of ammonia.

In the case of the scc-model, F represents the total number of monomers. Now we have $\exp(-\Delta G/kT) = 1$ for the monomers (1,0) and (0,1), and therefore we have to make a correction to using the Kronecker delta (see Kulmala *et al.*, 1992):

$$F_{\mathrm{scc}} = (1 - \delta_{0,nA}\delta_{0,nW})N_{A0} + (1 - \delta_{0,nA}\delta_{0,nW})N_{W0}, \tag{6}$$

which takes care of the fact that the number of monomer clusters cannot exceed the number of monomers.

The revised classical model

The revised classical model has mainly been adopted from Wilemski (see e.g. Wilemski, 1987).

The nucleation rate I can be calculated from equation (3). The Gibbs free energy at the saddle point is given as (within the framework of the capillarity approximation)

$$\Delta G^* = \tfrac{4}{3}\pi r^{*2}\sigma. \tag{7}$$

The critical radius r^* and the mole fraction at the saddle point can be determined from the Gibbs–Thomson equations, where the surface tension derivative is eliminated

$$kT \ln\frac{A_{ig}}{A_{il}} + \frac{2v_i\sigma}{r} = 0. \tag{8}$$

NUMERICAL CALCULATIONS AND THERMODYNAMIC DATA

In order to calculate the nucleation rate using the standard classical model and scc-model, we first have to determine $\Delta G(n_a, n_w, T)$ at the saddle point. We can construct a table of ΔG as a function of n_a and n_w and the "pass" in the ΔG "mountain" can be found by visual inspection or it can be calculated by a computer.

The second partial derivatives of ΔG are needed to determine the Zeldovich factor (in the present work in the standard and scc-model). They have been calculated with the following numerical equations (see e.g. Dahlquist and Björck, 1974; Kulmala *et al.*, 1991) at the point n_a, n_b.

The nucleation rate given by the revised model can be calculated using equations (3), (10) and (11). The direction of growth is estimated to be

$$\tan\phi = X. \tag{9}$$

This approximation has been shown to give growth angles similar to those given by a more rigorous expression (e.g. Kulmala and Laaksonen, 1990). The Zeldovich non-equilibrium factor is taken to be 0.05, which has been shown to give a reasonable estimation for Z (see e.g. Kulmala and Laaksonen, 1990).

To be able to calculate ΔG from the classical models one needs values for densities, activities, and surface tensions as functions of temperature.

The density of ammonia–water mixture experimental data (Landoldt-Börnstein, 1960) was correlated by

$$\rho_l = \rho_{Al}X^2 + \rho_{Wl}(1 - X)^2 + a_\rho X(1 - X) + b_\rho, \tag{10}$$

where ρ_{li} is the density of pure substance. The form of the correlation is purely artificial and the parameters a_ρ and b_ρ are fitted. They were found to be

$$a_\rho = 1686\ \mathrm{kg\,m^{-3}}, \qquad b_\rho = 11\ \mathrm{kg\,m^{-3}} \tag{11}$$

using the following correlation for the density of ammonia:

$$\rho_{Al} = 1065\ \mathrm{kg\,m^{-3}} - 1.613\ \mathrm{kg(m^{-3}\,K^{-1})}\,T, \tag{12}$$

where the temperature value T is given in degrees Kelvin. Expression is based on the experimental data (CRC Handbook, 1985). The density of pure water is calculated using the

correlation given by Kell (1975):

$$\rho_{w1} = (999.83952 + 16.945176T_c - 7.9870401 \times 10^{-3}T_c^2 - 46.170461 \times 10^{-6}T_c^3 + 105.56302 \times 10^{-9}T_c^4 - 280.54253 \times 10^{-12}T_c^5)/(1 + 16.879850 \times 10^{-3}T_c)\ \mathrm{kg\,m^{-3}} \quad (13)$$

where a temperature value T_c is given in degrees Celsius. The above correlation is presented in its original form, although it is much more accurate than needed in this study.

The relative error of the mixture density is 3% at the temperature interval from 0 to 60°C. However, in the model calculations the value of the mixture density is needed even at the temperature −70°C. At these temperatures there are no experimental data for the mixture density. For the density of pure water the value at the temperature −30°C is used also at the lower temperatures, because the correlation equation (Kell, 1975) does not extrapolate well below −30°C. Although very low droplet temperatures are considered, no ice formation exists in conditions treated in this study according to the phase diagram (see Landolt-Börnstein, 1960).

Partial vapour pressures above the surface of an ammonia solution are computed from the equation (see e.g. Reid *et al.*, 1987)

$$P_{i,sol} = \Gamma_i X_i p_{i,s}. \quad (14)$$

The saturation vapour pressure of pure ammonia (in Pascals) is based on the data given by Macriss *et al.* (1964):

$$p_{As} = \exp(58.0671 - 3967.8923/T - 5.6983 \ln T + 0.005T), \quad (15)$$

and the saturation vapour pressure for pure water (in Pascals) is (see Preining *et al.*, 1981)

$$p_{Ws} = \exp(77.34 - 7235/T - 8.2 \ln T + 0.005711T). \quad (16)$$

Note that the activity coefficients are below unity. The activity coefficients (Γ_i) used are given by Vesala and Kukkonen (1992).

The expression for the surface tension (in N/m) is based on the data given by Landolt-Börnstein (1960)

$$\sigma = (125.693 - 0.187439T + (161.601 - 0.764628T)X_m + (-198.813 + 0.724249T)X_m^2) \times 10^{-3}. \quad (17)$$

Here X_m is the mass fraction of ammonia in the droplet.

RESULTS AND DISCUSSION

The significance of droplet formation in the boundary layer of an evaporating ammonia droplet was simulated. The ambient relative humidity was 100%, and the ambient ammonia concentration was 0. The maximum temperature of stored ammonia was its boiling point at 1 atm. First, we compare different nucleation model to obtain numerically simple enough but still physically reliable model. Secondly, we used that model to estimate droplet formation in the diffusive boundary layer of an evaporating ammonia droplet.

Nucleation rates and nucleation onsets

The binary homogeneous nucleation of water–ammonia vapour system was simulated at different gas temperatures (223.15, 233.15 and 243.15 K). According to Vesala (1991) and the present simulations, these temperatures are typical in the boundary layers of an evaporating ammonia droplet. Water vapour gas-phase activity varied from 0.05 to 25. The ammonia gas-phase activity varied from 0.01 to 5. In the simulations we used the standard, the revised and the scc model of binary homogeneous nucleation.

The nucleation onset activities at different temperatures given by the three nucleation models are compared in Fig. 1. The lines represent a constant nucleation rate $10^6\ \mathrm{cm^{-3}\,s^{-1}}$

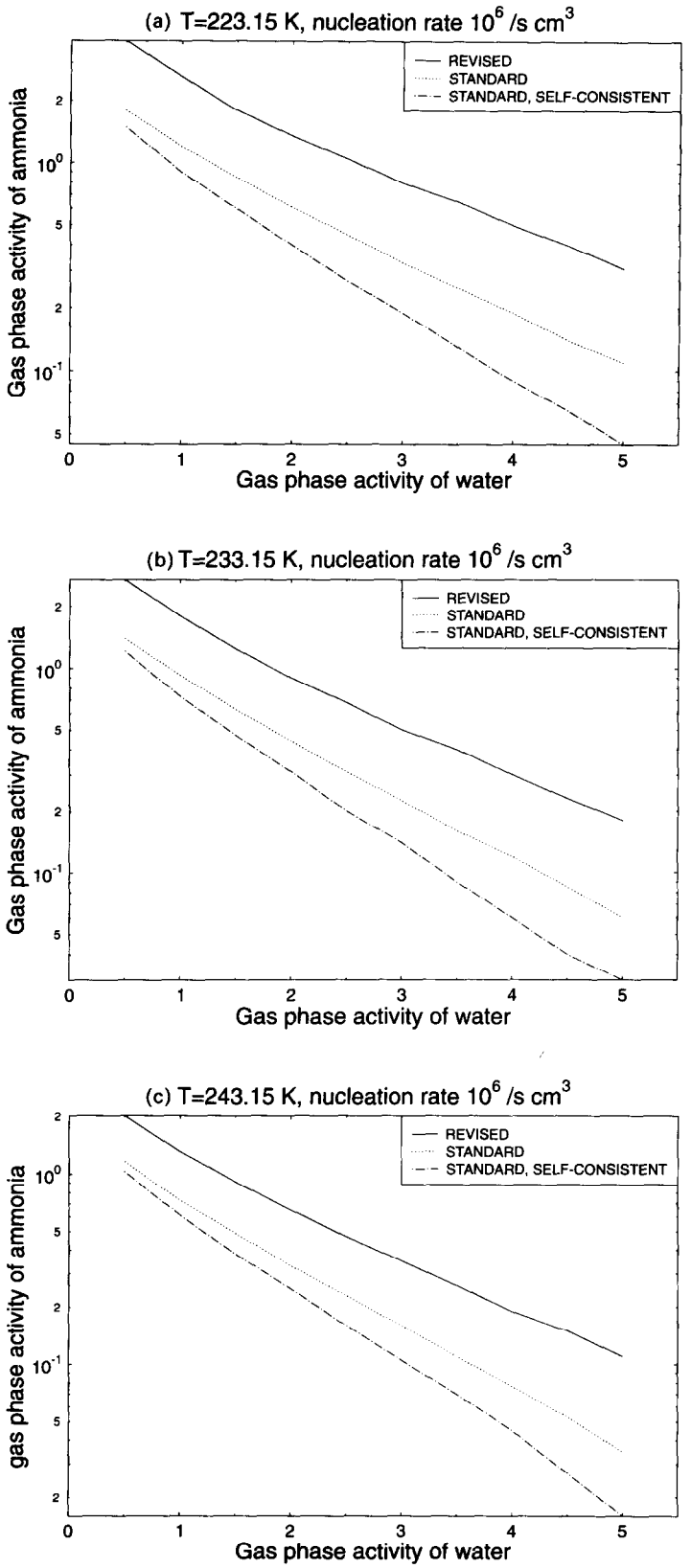

Fig. 1. The onset activities at nucleation rate of 10^6 cm^{-3} s^{-1} for water–ammonia system calculated by the revised, standard and scc models for binary homogeneous nucleation. T is 223.15 K (a), 233.15 K (b) and 243.15 K (c).

at three different temperatures 223.15, 233.15 and 243.15 K. The revised model needs significantly higher ammonia activities at the same water activity when compared to the other two models. The difference between the models will decrease, when water activity decreases. However, the curve is smooth and unphysical behaviour, which the revised model predicts for some systems (for example, water–alcohol systems) (see e.g. Wilemski, 1987; Laaksonen *et al.*, 1993) does not appear. This enables us to use (as a next step) the revised theory in the model, where aerosol dynamics in the boundary layer is simulated. There are

Table 1. Nucleation rates I ($cm^{-3}s^{-1}$) as a function of temperature (T) and gas-phase activities A_{Ag} for ammonia and A_{Wg} for water. The critical radius (r^*), the critical energy barrier ($\Delta G/kT$) and corresponding mole fraction X

T (K)	A_{Ag}	A_{Wg}	r^* (m)	X	$\Delta G/kT$	I ($cm^{-3}s^{-1}$)
233.15	0.30	1	0.110×10^{-8}	0.338	0.116×10^{3}	0.469×10^{-26}
233.15	0.30	2	0.833×10^{-9}	0.294	0.676×10^{2}	0.153×10^{-4}
233.15	0.30	3	0.724×10^{-9}	0.269	0.516×10^{2}	0.194×10^{3}
233.15	0.30	4	0.661×10^{-9}	0.253	0.433×10^{2}	0.101×10^{7}
233.15	0.30	5	0.619×10^{-9}	0.240	0.381×10^{2}	0.226×10^{9}
233.15	0.30	6	0.588×10^{-9}	0.230	0.345×10^{2}	0.101×10^{11}
233.15	0.30	7	0.563×10^{-9}	0.222	0.318×10^{2}	0.174×10^{12}
233.15	0.30	8	0.544×10^{-9}	0.215	0.297×10^{2}	0.163×10^{13}
233.15	0.30	9	0.527×10^{-9}	0.209	0.280×10^{2}	0.100×10^{14}
233.15	0.30	10	0.513×10^{-9}	0.204	0.266×10^{2}	0.454×10^{14}
233.15	0.30	11	0.501×10^{-9}	0.199	0.254×10^{2}	0.164×10^{15}
233.15	0.30	12	0.491×10^{-9}	0.194	0.244×10^{2}	0.497×10^{15}
233.15	0.30	13	0.481×10^{-9}	0.190	0.235×10^{2}	0.131×10^{16}
233.15	0.30	14	0.473×10^{-9}	0.187	0.227×10^{2}	0.309×10^{16}
233.15	0.30	15	0.465×10^{-9}	0.183	0.220×10^{2}	0.666×10^{16}
233.15	0.30	16	0.458×10^{-9}	0.180	0.214×10^{2}	0.133×10^{17}
233.15	0.30	17	0.452×10^{-9}	0.177	0.208×10^{2}	0.249×10^{17}
233.15	0.30	18	0.446×10^{-9}	0.174	0.203×10^{2}	0.441×10^{17}
233.15	0.30	19	0.441×10^{-9}	0.172	0.198×10^{2}	0.746×10^{17}
233.15	0.30	20	0.436×10^{-9}	0.169	0.194×10^{2}	0.121×10^{18}
233.15	0.30	21	0.431×10^{-9}	0.167	0.190×10^{2}	0.190×10^{18}
233.15	0.30	22	0.427×10^{-9}	0.165	0.186×10^{2}	0.288×10^{18}
233.15	0.30	23	0.423×10^{-9}	0.163	0.183×10^{2}	0.425×10^{18}
233.15	0.30	24	0.419×10^{-9}	0.160	0.180×10^{2}	0.612×10^{18}
233.15	0.30	25	0.415×10^{-9}	0.159	0.177×10^{2}	0.863×10^{18}

T (K)	A_a	A_w	r^* (m)	X	$\Delta G/kT$	I ($cm^{-3}s^{-1}$)
233.15	0.60	1	0.917×10^{-9}	0.375	0.788×10^{2}	0.217×10^{-9}
233.15	0.60	2	0.733×10^{-9}	0.327	0.516×10^{2}	0.277×10^{3}
233.15	0.60	3	0.652×10^{-9}	0.301	0.413×10^{2}	0.114×10^{8}
233.15	0.60	4	0.604×10^{-9}	0.284	0.357×10^{2}	0.428×10^{10}
233.15	0.60	5	0.570×10^{-9}	0.270	0.320×10^{2}	0.212×10^{12}
233.15	0.60	6	0.545×10^{-9}	0.260	0.294×10^{2}	0.355×10^{13}
233.15	0.60	7	0.525×10^{-9}	0.251	0.273×10^{2}	0.308×10^{14}
233.15	0.60	8	0.509×10^{-9}	0.244	0.258×10^{2}	0.172×10^{15}
233.15	0.60	9	0.495×10^{-9}	0.237	0.244×10^{2}	0.710×10^{15}
233.15	0.60	10	0.483×10^{-9}	0.232	0.234×10^{2}	0.234×10^{16}
233.15	0.60	11	0.473×10^{-9}	0.227	0.224×10^{2}	0.653×10^{16}
233.15	0.60	12	0.464×10^{-9}	0.222	0.216×10^{2}	0.159×10^{17}
233.15	0.60	13	0.456×10^{-9}	0.218	0.209×10^{2}	0.350×10^{17}
233.15	0.60	14	0.449×10^{-9}	0.214	0.203×10^{2}	0.705×10^{17}
233.15	0.60	15	0.443×10^{-9}	0.210	0.197×10^{2}	0.132×10^{18}
233.15	0.60	16	0.437×10^{-9}	0.207	0.192×10^{2}	0.234×10^{18}
233.15	0.60	17	0.431×10^{-9}	0.204	0.188×10^{2}	0.393×10^{18}
233.15	0.60	18	0.426×10^{-9}	0.201	0.183×10^{2}	0.633×10^{18}
233.15	0.60	19	0.421×10^{-9}	0.198	0.179×10^{2}	0.983×10^{18}
233.15	0.60	20	0.417×10^{-9}	0.196	0.176×10^{2}	0.148×10^{19}
233.15	0.60	21	0.413×10^{-9}	0.193	0.173×10^{2}	0.215×10^{19}
233.15	0.60	22	0.409×10^{-9}	0.191	0.170×10^{2}	0.307×10^{19}
233.15	0.60	23	0.405×10^{-9}	0.189	0.167×10^{2}	0.427×10^{19}
233.15	0.60	24	0.402×10^{-9}	0.187	0.164×10^{2}	0.582×10^{19}
233.15	0.60	25	0.399×10^{-9}	0.185	0.161×10^{2}	0.779×10^{19}

three reasons to use the revised model: (i) it is thermodynamically consistent (see Wilemski, 1987); (ii) it is the numerically easiest one; and (iii) it gives a conservative estimate on nucleation onset, since it gives smaller nucleation rates than other models.

Results of calculations using the revised theory in Table 1 show that the physical diameter of critical clusters is about 1 nm. When the nucleation rate is about 1 $cm^{-3}s^{-1}$ (which is the so called critical (onset) nucleation rate for nucleation experiments in thermal diffusion chambers), the mole fraction of ammonia molecules varies from 0.1 to 0.4. The critical energy barrier at the saddle point depends on gas-phase activities and temperature. However, it is 50–60 kT for the onset nucleation rate.

Ammonia clearly enhances the nucleation rate, when compared with homomolecular water nucleation (see Fig. 2). The needed water gas-phase activity for significant nucleation decreases from 10 to about 5 when the ammonia activity increases from 0 to 0.3. As an overall result we can see that a small rise in NH_3 or water gas-phase activity increases the nucleation rate considerably throughout the whole range of simulations.

Nucleation in the boundary layer

Nucleation rates in the boundary layer are simulated using the revised nucleation theory, and are calculated as a function of radial position. Temperatures and vapour concentrations are estimated using hyperbolic zeroth-order temperature and vapour profiles (see e.g. Seinfeld, 1986). An example of our simulations is presented in Fig. 3. The nucleation rate has a peak near the distance 1.2 radius from the centre of an evaporating droplet. The water saturation has its maximum near the same place as the nucleation rate. The temperature increases slightly and ammonia saturation decreases as a function of radial distance.

The radius of the evaporating ammonia droplet is around 100 μm. Using Fig. 3 it is possible to estimate the volume, where the nucleation can occur. This volume is *ca* 10^{-12} m^3. To estimate if nucleation is significant or not the time for nucleation event has to be estimated.

As the nucleated droplets grow, the water and ammonia gas-phase activities fall until the nucleation rate becomes negligible. The time for this to happen is termed the cutoff time t_c and can be estimated using a similar procedure to that used in the unary case by Barrett and Clement (1991). The extension of their treatment to the binary case is outlined in the appendix. One significant difference is that, due to the much larger binary nucleation rates, droplets do not grow out of the free molecular growth regime before nucleation is cutoff.

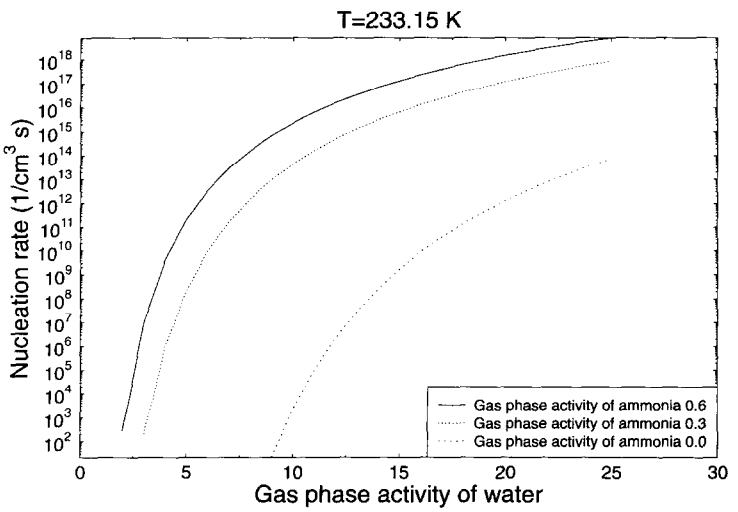

Fig. 2. The nucleation rate in water–ammonia system as a function of water activity calculated by the revised model for binary homogeneous nucleation. T is 233.15 K.

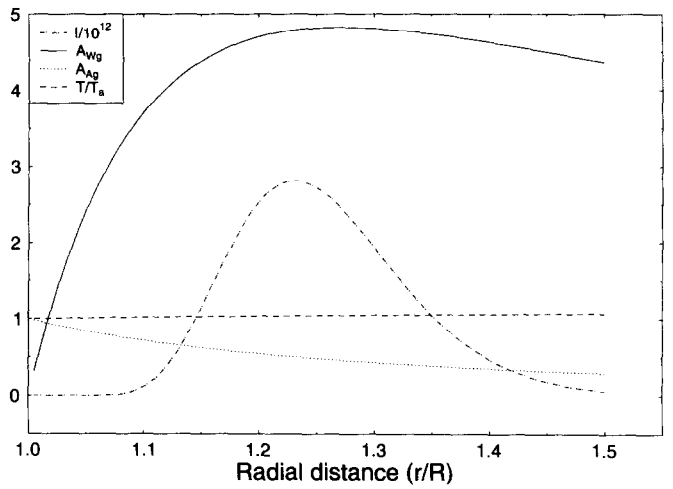

Fig. 3. Nucleation rate (in units 10^{12} cm^{-3} s^{-1}), temperature divided by the droplet temperature and gas-phase activities of water and ammonia as a function of radial distance. The droplet temperature is 233.15 K and the ambient temperature 283.15 K. The ambient relative humidity is 100%. The ambient ammonia concentration is 0. The mole fraction of water at the droplet surface is 0.

Once t_c is known, the total number of droplets nucleated per m^3 at position r in the boundary layer can be found from $N(r) = It_c$. In Fig. 4, the number nucleated per micrometer of boundary layer, i.e. $4\pi r^2 N(r) \times 10^{-6}$, is shown. The area under this curve gives the total number of droplets nucleated throughout the boundary layer (about 22,000 when the ambient temperature is 283.15 K). The maximum number nucleated per m^3 in the boundary layer (i.e. the value of N, where $dN/dr = 0$) for various ambient temperatures is shown in Fig. 5. Also shown is the corresponding cutoff time t_c.

These results span the ambient temperature region where mixed droplets would really nucleate, grow and emerge from the boundary layer around a large (100 μm) ammonia drop. Droplet motion would arise from the combination of thermophoresis, directed towards the ammonia drop, and diffusiophoresis from the ammonia current away from the drop and a much smaller (factor 10–100) water vapour current towards the drop. According to our previous estimates (Barrett *et al.*, 1992), the diffusiophoretic velocity would be larger, although the thermophoretic velocity would be comparable at a low temperature (– 60°C), and the net outward droplet velocity would range from about 0.095 m s^{-1} at $T_a = -40$°C to 0.027 m s^{-1} at $T_a = -50$°C, the corresponding transit times for nucleating droplets to emerge from a 20 μm wide growth zone would be 0.2 and 0.75 ms, respectively. At the lower temperatures shown in Fig. 5, their growth would fail to cut off nucleation, a failure reinforced by diffusion of the two vapours which would tend to maintain original water and ammonia activities.

Actual nucleation rates would not have a significant effect on the boundary layer until they produced about 1 droplet ms^{-1} which, for a thickness, ΔR of about 20 μm at $R = 10^{-4}$ m, corresponds to a nucleation rate of

$$I = \frac{1/\text{ms}}{4\pi R^2 \Delta R} = 4 \times 10^{14} \text{ m}^{-3} \text{s}^{-1}. \tag{18}$$

In spite of the large uncertainties in the calculations, the results shown in Fig. 5 suggest that large numbers of droplets would appear as the ambient temperature rises a few degrees above 10°C.

A full description of droplet nucleation, subsequent motion and growth, and their coupling to the ammonia and water vapour currents has not been attempted here because of its complexity, although we hope to pursue the subject in future. A steady state could be

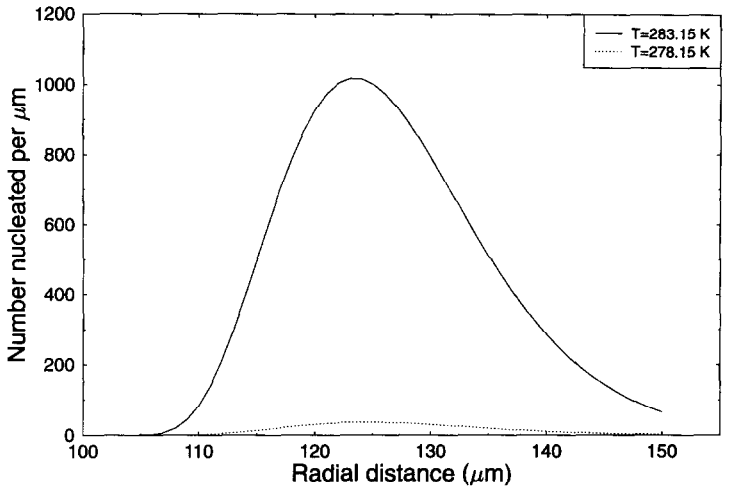

Fig. 4. Variation of number nucleated per μm in boundary layer, $4\pi N \times 10^{-6}$, with radial distance $r(\mu m)$ at the ambient temperatures 283.15 and 278.15 K. Other conditions are as in Fig. 3.

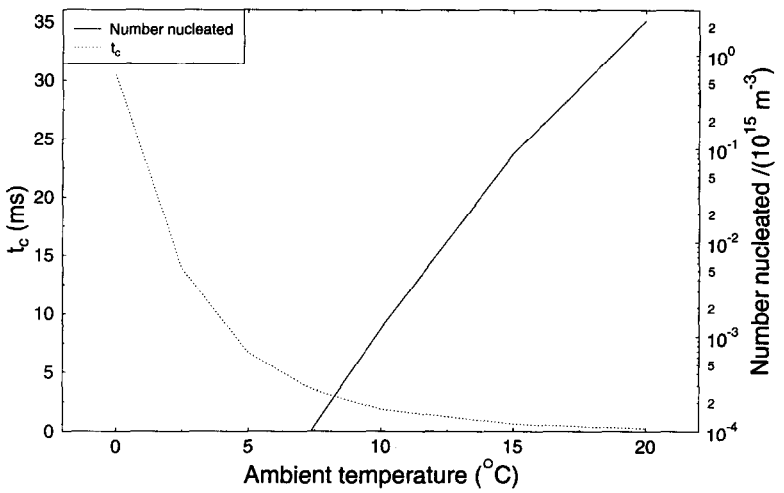

Fig. 5. Variation of the maximum number of droplets nucleated per m^3 in the boundary layer with ambient temperature (in °C). The droplet temperature is 233.15 K. Also shown is the cutoff time, t_c in ms.

reached if droplet motion removes droplets faster than nucleation is cut off by vapour depletion, as calculated here. Droplet coagulation is not likely to be important in the physical processes involved because its longer timescale, given for the dominant Brownian coagulation of equal-sized droplets by

$$\tau_B = \frac{3\mu}{4kTN}, \tag{19}$$

where μ is the gas viscosity. With gas viscosities for air in the range $1.5\text{–}1.6 \times 10^{-5}$ kg(m s^{-1}) for $T = -20$ to -40°C, τ_B is practically independent of temperature over the range, and, for the maximum value of $N = 10^{15}$ m^{-3} s^{-1} shown in Fig. 5, only reaches its lowest value of $\tau_B = 3.6$ s, much longer than the estimated boundary layer transit times of < 0.1 s.

The actual nucleation rate depends on the droplet temperature, ambient temperature, ambient humidity and the mole fractions at the droplet surface. Table 2 summarizes the

Table 2. Nucleation in the boundary layer

T_a (K)	T_∞ (K)	r/R	$A_{w,max}$	$A_{a,max}$	$T_{N,max}$	I_{max}
239.25	253.15	–	–	–	–	–
239.25	273.15	1.28	1.89	0.54	246.66	0.40×10^{5}
239.25	293.15	1.23	4.86	0.50	249.33	0.10×10^{15}
238.15	253.15	–	–	–	–	–
238.15	273.15	1.28	2.05	0.54	245.81	1.9×10^{5}
238.15	293.15	1.23	5.29	0.49	248.43	0.21×10^{15}
233.15	253.15	1.37	1.03	0.55	238.55	0.15×10^{-8}
233.15	273.15	1.25	2.90	0.53	241.15	0.10×10^{9}
233.15	293.15	1.22	7.65	0.47	243.97	0.34×10^{16}
223.15	253.15	1.28	2.08	0.54	229.97	0.84×10^{1}
223.15	273.15	1.22	6.44	0.49	232.17	0.12×10^{13}
223.15	293.15	1.20	17.31	0.43	234.82	0.26×10^{18}
213.15	253.15	1.23	4.91	0.51	220.63	0.22×10^{8}
213.15	273.15	1.20	15.94	0.45	223.15	0.70×10^{15}
213.15	293.15	1.19	42.75	0.38	225.92	0.52×10^{19}
203.15	253.15	1.20	13.47	0.47	211.48	0.32×10^{12}
203.15	273.15	1.18	44.58	0.41	213.83	0.50×10^{17}
203.15	293.15	1.18	116.96	0.33	216.88	0.40×10^{20}

T_a and T_∞ are the droplet temperature and the ambient temperature, respectively. Ambient relative humidity is 100%. The ambient ammonia concentration is 0. The ammonia mole fraction at the surface is 1. r/R is the radial position divided by the droplet radius. I_{max} is the maximum nucleation rate ($cm^{-3} s^{-1}$) in the boundary layer. $A_{i,max}$ are the corresponding gas-phase activities. $T_{N,max}$ is the corresponding temperature.

results of our simulations. The droplet temperature varies from the boiling point of ammonia to $-70°C$. If the mole fraction of ammonia at the surface of the evaporating droplet is 1, a temperature difference of about 40°C (ambient relative humidity 100%) is needed to obtain significant nucleation. We have also considered the case, when the ammonia mole fraction is 0.1. Then the temperature difference needed is near 50°C.

CONCLUSIONS

The binary homogeneous nucleation in NH_3–water system will take place more easily than homomolecular water nucleation. The results obtained from the different classical nucleation models differ clearly from each other. However, the unphysical behaviour, which is typical for revised nucleation theory for some systems, does not occur for water–ammonia system. This shows that the NH_3–water system behaves similarly to water–acid (e.g. sulphuric acid, nitric acid) systems.

In the view of our results we predict that water–ammonia nucleation is very probable in the boundary layer of evaporating ammonia droplet and that nucleated droplets would emerge from the boundary layer. The temperature difference needed for significant nucleation is *ca* 40–50°C, if the ambient relative humidity is 100%. This is the condition which can be reached during accidental releases of pressurised ammonia. The question whether the homogeneous nucleation plays any relevant role in overall dynamics of those releases remains to be quantified in the future.

Acknowledgements—Support of this work by the Academy of Finland is gratefully acknowledged.

REFERENCES

Barrett, J. C. and Clement, C. F. (1991) Aerosol concentrations from a burst of nucleation. *J. Aerosol Sci.* **22**, 327–335.

Barrett, J. C., Clement, C. F., Kulmala, M. and Vesala, T. (1992) The physics of aerosol formation in diffusive boundary layers. *J. Aerosol Sci.* **23**, S121–S124.
CRC (1979) *Handbook of Chemistry and Physics*, 60th Edition. The Chemical Rubber Co, Cleveland, OH.
Dahlquist, G. and Björck, Å. (1974) *Numerical Methods*. Prentice-Hall, Englewood Cliffs, NJ.
Heist, R. H. and Reiss, H. (1974) Hydrates in supersaturated binary sulfuric acid–water vapor. *J. chem. Phys.* **61**, 573.
Kell, G. S. (1975) Density, thermal expansivity and compressibility of liquid water from 0°C to 150°C: correlations and tables for atmospheric pressure and saturation reviewed and expressed on 1968 temperature scale. *J. chem. Engng Data* **20**, 97–105.
Kukkonen, J. (1990) Modelling source terms for atmospheric dispersion of hazardous substances. Ph.D. thesis, Commentationes Physico- Mathematicae, 115. The Finnish Society of Sciences and Letters, Helsinki.
Kukkonen, J., Vesala, T. and Kulmala, M. (1989) The interdependence of evaporation and settling for airborne freely falling droplets. *J. Aerosol Sci.* **20**, 749–763.
Kulmala, M. and Laaksonen, A. (1990) Binary nucleation of water—sulphuric acid system: comparison of classical theories with different H_2SO_4 saturation vapour pressures. *J. chem. Phys.* **93**, 696.
Kulmala, M., Laaksonen, A. and Jokiniemi, J. (1991) Numerical simulation of binary nucleation of hydrogen iodide and water vapours. *J. Aerosol Sci.* **22**, 149–157.
Kulmala, M., Laaksonen, A. and Girshick, S. L. (1992) The self-consistency correction to homogeneous nucleation: extension to binary systems. *J. Aerosol Sci.* **23**, 309–312.
Kulmala, M., Vesala, T. and Wagner, P. E. (1993) An analytical expression for the rate of binary condensational particle growth. *Proc. R. Soc. London A* **441**, 589–605.
Laaksonen, A., Kulmala, M. and Wagner, P. E. (1993) On the cluster compositions in the classical binary nucleation theory. *J. chem. Phys.* **99**, 6832–6835.
Landolt-Börnstein (1960) *Zahlenwerte und Functionen aus Physik- Chemie-Astronomie-Geophysik-Technik*. Springer, Berlin.
Macriss, R. A., Eakin, B. E., Ellington, R. T. and Huebler, J. (1964) Physical and thermodynamic properties of ammonia–water mixtures. Institute of Gas Technology, Research Bulletin 34, Chicago, IL.
Preining, O., Wagner, P. E., Pohl, F. G. and Szymanski, W. (1981) *Heterogeneous Nucleation and Droplet Growth*, 269 pp. University of Vienna, Institute of Experimental Physics, Vienna.
Reid, R. C., Prausnitz, J. M. and Poling, B. E. (1987) *The Properties of Gases and Liquids*, 4th Edition. McGraw-Hill, New York.
Reiss, H. (1950) The kinetics of phase transitions in binary systems. *J. chem. Phys.* **18**, 840.
Seinfled, J. H. (1986) *Atmospheric Chemistry and Physics of Air Pollution*. Wiley, New York.
Stauffer, D. (1976) Kinetic theory of two-component (hetromolecular) nucleation and condensation. *J. Aerosol Sci.* **7**, 319.
Vesala, T. (1991) Binary droplet evaporation and condensation as phenomenological processes. Commentationes Physico-Mathematicae et Chemico-Medicae 127.
Vesala, T. and Kukkonen, J. (1992) A model for binary droplet evaporation and condensation, and its application for ammonia droplets in humid air. *Atmos. Envir.* **26A**, 1573–1581.
Wilemski, G. (1987) Revised classical binary nucleation theory for aqueous alcohol and acetone vapors. *J. phys. Chem.* **91**, 2492.
Yue, G. K. and Hamill, P. (1979) The homogeneous nucleation rates of H_2SO_4–H_2O aerosol particles in air. *J. Aerosol Sci.* **10**, 609.

APPENDIX: CALCULATION OF CUTOFF TIME

The mass flux of water vapour condensing on a single droplet of radius R (assuming that the mass fractions of water and ammonia in the growing droplets remain constant) is (from Kulmala *et al.*, 1993)

$$F_W = 4\pi R^2 \frac{dR}{dt}(1 - X_m)\rho_l = \frac{4\pi R^2}{R_G T}\left(\frac{\frac{1}{4}M_W \bar{c}_W (A_{Wg} - A_{Wl})}{1 + \theta}\right), \tag{A1}$$

with

$$\theta = \frac{(1 - X_m)L_W + X_m L_A}{K R_G^2 T^3}(\tfrac{1}{4}L_W M_W^2 \bar{c}_W p_{Ws} A_{Wl} + (\tfrac{1}{4}L_A M_A^2 \bar{c}_A p_{As} A_{Al}), \tag{A2}$$

where K is the thermal conductivity of the vapour–gas mixture and M_i, L_i, $\bar{c}_i$ are the molecular mass, latent heat, and mean molecular speed of species i. R_G is the general gas constant.

Our main assumption is that the gas-phase activities (and therefore also the nucleation rate I) remain constant up to t_c and then fall instantaneously by amounts ΔA_{Ag}, ΔA_{Wg} which reduces I by a factor e. Then equation (A1) can be integrated to give

$$R(t) = \frac{\frac{1}{4}M_W \bar{c}_W p_{Ws}(A_{Wg} - A_{Wl})t}{(1 - X_m)\rho_l(1 + \theta)}. \tag{A3}$$

Since the nucleation rate is assumed to be constant, the water condensation rate per unit volume is

$$\dot{m}_W = \tfrac{4}{3}\pi R^3(t)\rho_l(1 - X_m)I. \tag{A4}$$

Using equation (A3) into equation (A4) and integrating gives the total mass of water condensed per unit volume in time t_c as

$$\Delta m_W = \tfrac{4}{3}\pi I \rho_l (1 - X_m)\left(\frac{\tfrac{1}{4}M_W \bar{c}_W (A_{Wg} - A_{Wl})}{(1 - X_m)\rho_l (1 + \theta)}\right)^{\frac{1}{4}} t_c^4. \tag{A5}$$

To relate the change in gas-phase activity ΔA_{Wg} to Δm_w it is necessary to consider the energy and liquid–vapour mass balance equations for the mixture. The procedure is essentially identical to that used in the unary case (Barrett and Clement, 1991) and the result is

$$\Delta A_{Wg} = \frac{-1}{\rho_{Ws}}\left(1 + \frac{L_W \rho'_{Ws} A_{Wg}}{\rho c_p}\right)\Delta m_W - \frac{A_{Wg}\rho'_{Ws} L_A \Delta m_A}{\rho c_p}, \tag{A6}$$

where ρc_p is the heat capacity of the mixture (taken to be that of pure air) and ρ'_{Ws} denotes the temperature derivative of the equilibrium water vapour density, ρ_{Ws}. The term proportional to Δm_A arises because the latent heat of ammonia condensation affects the mixture temperature.

Since the mass fractions in the droplets are assumed constant, it follows that $(1 - X_m)\Delta m_A = X_m \Delta m_W$. Using this and substituting equation (A5) into equation (A6) gives $\Delta A_{Wg} = -\lambda_W t_c^4$, where

$$\lambda_W = \frac{1}{\rho_{Ws}}\left[1 + \frac{\rho'_{Ws} A_{Wg}}{\rho c_p}\left(L_W + \frac{L_A X_m}{(1 - X_m)}\right)\right] \times \frac{\pi}{3} I \rho_l (1 - X_m)\left(\frac{\tfrac{1}{4}M_W \bar{c}_W (A_{Wg} - A_{Wl})}{(1 - X_m)\rho_l (1 + \theta)}\right)^3. \tag{A7}$$

The same procedure for the ammonia component gives $\Delta A_{Ag} = -\lambda_A t_c^4$, where λ_A is given by equation (A7) with the subscripts A and W interchanged.

Finally, the changes in A_{Wg} and A_{Ag} require to reduce the nucleation rate by a factor e satisfy

$$\frac{\partial \ln I}{\partial A_{Wg}}\Delta A_{Wg} + \frac{\partial \ln I}{\partial A_{Ag}}\Delta A_{Ag} = -1, \tag{A8}$$

and therefore

$$t_c = \left[\lambda_W \frac{\partial \ln I}{\partial A_{Wg}} + \lambda_A \frac{\partial \ln I}{\partial A_{Ag}}\right]^{-1/4}. \tag{A9}$$

In numerical calculations, the derivatives in equation (A9) were determined by finite differencing.